N O T I C E

THIS DOCUMENT HAS BEEN REPRODUCED FROM
MICROFICHE. ALTHOUGH IT IS RECOGNIZED THAT
CERTAIN PORTIONS ARE ILLEGIBLE, IT IS BEING RELEASED
IN THE INTEREST OF MAKING AVAILABLE AS MUCH
INFORMATION AS POSSIBLE

CORNELL UNIVERSITY

Center for Radiophysics and Space Research

ITHACA, N. Y.

EFFECTS OF TRUNCATION IN

MODAL REPRESENTATIONS OF THERMAL CONVECTION

Philip S. Marcus

EFFECTS OF TRUNCATION IN

MODAL REPRESENTATIONS OF THERMAL CONVECTION*

Philip S. Marcus

Center for Radiophysics and Space Research

Cornell University

November 1979

ABSTRACT

We examine the Galerkin (including single-mode and Lorenz) equations for convection in a sphere to determine which physical processes are neglected when the equations of motion are truncated too severely. We test our conclusions by calculating solutions to the equations of motion for different values of the Rayleigh number and for different values of the limit of the horizontal spatial resolution. We show that the transitions from steady-state to periodic, then to aperiodic convection depend not only on the Rayleigh number but also very strongly on the horizontal resolution. All of our models are well-resolved in the vertical direction, so the transitions do not appear to be due to poorly resolved boundary-layers. One of the effects of truncation is to enhance the high wavenumber end of the kinetic energy and thermal variance spectra. Our numerical examples indicate that as long as the kinetic energy spectrum decreases with wavenumber, a truncation gives a qualitatively correct solution.

I. INTRODUCTION

In Rayleigh-Bernard convection, discrete transitions from steady-state to periodic to aperiodic convection have been experimentally observed. (See the recent reviews by Fenstermacher et al. 1978 and Busse 1978.) As the Rayleigh number is increased and the fluid becomes more "turbulent", the Fourier spectrum (in time) of the velocity develops a single spike (and its overtones) and shows a gradual increase of the broad band background noise that eventually overwhelms the spikes. Although the transitions depend not only on the Rayleigh number but also on the Prandtl number and initial conditions, there has recently been much interest in trying to compute these transitions from the actual equations of motion.

In attempting to compute time-dependent numerical solutions to the three-dimensional Navier-Stokes equation, one is forced to make severe approximations. When simplifying the equations of motion to make them numerically tractable, one hopes to establish a compromise so that the modified equations are uncomplicated enough to be easily solved, yet complete enough that the underlying physics of the fluid dynamics is not lost.

The crudest approximation is the Lorenz (1963) model. The Lorenz model predicts not only the transitions to steady-state and time-dependent convection, but also a sequence of bifurcations that eventually leads to chaotic (aperiodic) behavior. For low Rayleigh numbers near the onset of convection the heat flux (Nusselt number) predicted by the Lorenz model is in fair

agreement with laboratory results. As the Rayleigh number increases,
the calculated and experimentally observed Nusselt numbers begin
to differ. When the Rayleigh number is as large as the one at
which the Lorenz model predicts a transition to chaos, there is
an appreciable difference between theoretical and experimental
values of the heat flux and one must seriously question the quali-
tative behavior of the time-dependency of the solution. McLaughlin
and Martin (1975) have expanded the Lorenz model to four inter-
acting modes and have found support of the Rouelle-Takens (1971)
theory of turbulence, which states that after no more than three
bifurcations to a periodic or quasi-periodic state there should
be a transition to aperiodicity. The fundamental question to be
answered, of course, is whether the qualitative time dependence
of these equations is due to the underlying physics that these
equations are trying to model or whether bifurcations are a
general property of sets of severely truncated nonlinear differen-
tial equations. A truncation of the governing equations of con-
vection that is less severe than McLaughlin and Martin's treat-
ment in the radial direction is single-mode theory (Gough et al.,
1975). Single-mode theory has only one horizontal mode
so has less horizontal resolution than McLaughlin and Martin's
4-mode solution. Surprisingly, the numerical solutions to the
single-mode equations (Toomre et al., 1977) do not exhibit bifur-
cations to periodic or aperiodic states and are time-independent
for all Rayleigh numbers. Numerical solutions to a truncated
Galerkin expansion of the equations of convection that is less
severe than both single-mode theory and McLaughlin and Martin's

equations have been computed by this author (Marcus 1980a, 1980b),
in which not just one but several horizontal modes of the expan-
sion are retained. For steady-state convection the results are
in good agreement with single-mode calculations. However, at lar-
ger Rayleigh numbers we find that the solutions become periodic
in time and, as the Rayleigh number is increased further, aperio-
dic in time. For some Rayleigh numbers that produce steady-
state solutions, we find (holding the Rayleigh number and the
resolution in the radial direction fixed) that as we decrease
the number of horizontal modes in the Galerkin expansion, there
is a transition from steady-state convection to a solution that
is periodic in time. As the number of modes is decreased still
further, the solutions become aperiodic. Obviously, the bifur-
cations depend not only on the Rayleigh number, Prandtl number
geometry and initial conditions, but also on the horizontal
resolution of the equations of motion.

In trying to understand mathematically the bifurcation
sequence of a truncated representation of the equations of motion,
it is easy to lose sight of what is physically happening in
the fluid. Therefore, the purpose of this paper is to examine
the solutions to truncated modal equations for convection in a
sphere and to determine which qualitative features of the solu-
tions represent real physical processes in the fluid and which
features are due solely to the effects of truncation.

In section 2 of this paper we briefly review the Galerkin
multi-mode equations (including single-mode and Lorenz) for

spherical convection. We attempt to describe the physics that
each system of equations models, which physical processes are
neglected by the various truncation schemes, and what artifi-
cial constraints each model imposes on its solutions. In the
third section we present the results of our multi-mode calcula-
tions for two different values of the Rayleigh number. For
each Rayleigh number we compute several models, each with a
different degree of horizontal truncation. By computing how
the energy spectra, convective flux, and temperature gradient
change as a function of the severity of truncation, we provide
a possible explanation for the time-dependence of our solutions.
Our conclusions appear in section 4.

<div align="center">

II. APPROXIMATIONS NEEDED FOR THE LORENZ,
SINGLE-MODE AND MULTI-MODE MODELS

</div>

Convection in a Boussinesq fluid is governed by the Navier-
Stokes, continuity and   thermal diffusion equations, and the
Boussinesq equation of state. (See, for example, Chandrasekhar,
1961). A standard technique used to simplify these coupled,
nonlinear, partial differential equations is the Galerkin method.
The thermodynamic quantities and velocity are expanded as an
infinite sum of coefficients multiplied by orthonormal functions
and substituted into the governing equations. Then, depending
on how many of the coefficients are solved   and how many are
arbitrarily set equal to zero, one arrives at a Lorenz, single-
mode, or multi-mode model.

A) Review of the Multi-Mode Equations

Let us consider convection in a self-gravitating sphere of Boussinesq fluid with thermal expansion coefficient α, heat capacity C_p, kinematic viscosity ν, thermal diffusivity k, radius d, and a heat source $H(r)$ in the fluid. Each scalar quantity, such as the temperature, is written as a sum of its mean, $\langle T(r,t)\rangle$, and fluctuating, $T(r,\theta,\phi,t)$, parts where

$$\langle T(r,t)\rangle = \int_{4\pi} T(r,\theta,\phi,t)\, d\Omega/4\pi \tag{2.1}$$

and

$$\tilde{T}(r,\theta,\phi,t) = 2(2\pi)^{1/2} \sum_{\ell=1}^{\infty} \left\{ \sum_{m=1}^{\ell} [T_{R,\ell,m}(r,t)\, \mathrm{Re}(Y^{\ell,m}) \right.$$
$$+ T_{I,\ell,m}(r,t)\, \mathrm{Im}(Y^{\ell,m})]$$
$$\left. + 2^{-1/2}\, T_{R,\ell,o}(r,t)\, Y^{\ell,o} \right\}, \tag{2.2}$$

$\mathrm{Re}(Y^{\ell,m})$ and $\mathrm{Im}(Y^{\ell,m})$ are the real and imaginary parts of the of the spherical harmonic. The velocity is written as a sum of its poloidal $\underline{v}_p$ and toroidal $\underline{v}_T$ parts which are derived from scalar fields ω and ψ

$$\underline{v}_p = \nabla\,[\partial(r\omega)/\partial r] - (r\nabla^2\omega)\,\hat{e}_r \tag{2.3}$$

$$\underline{v}_T = r\nabla \times (\psi\hat{e}_r) \tag{2.4}$$

Substituting expressions (2.3) and (2.4) into the equations of motion yields the equations for the coefficients for the temperature, T, pressure, P, gravitational potential, ϕ, and velocity, $\underline{v}$ (Marcus, 1980a):

$$\partial \omega_{\gamma,\ell,m} / \partial t =$$

$$-r \, [\ell(\ell+1)]^{-1} \, [R_s Pr \, r \, T_{\gamma,\ell,m} + \partial \, (P_{\gamma,\ell,m} + \Phi_{\gamma,\ell,m})/\partial r]$$

$$+ Pr \, \mathcal{D}_\ell \; (\omega_{\gamma,\ell,m})$$

$$- \ell(\ell+1)^{-1} \, \{r \, \hat{e}_r \cdot [(\underline{v}\cdot\nabla)\underline{v}]\}_{\gamma,\ell,m} \tag{2.5}$$

$$\partial \psi_{\gamma,\ell,m}/\partial t = Pr \, \mathcal{D}_\ell \; (\psi_{\gamma,\ell,m})$$

$$-\ell(\ell+1)^{-1} \, \{r \, \hat{e}_r \cdot \nabla \times [\underline{v}\cdot\nabla)\underline{v}]\}_{\gamma,\ell,m} \tag{2.6}$$

$$\partial \, T_{\gamma,\ell,m} / \partial t = \mathcal{D}_\ell \; (T_{\gamma,\ell,m})$$

$$- \ell(\ell+1) \, (\partial \langle T\rangle/\partial r) \, \omega_{\gamma,\ell,m}/r$$

$$- [\underline{v} \cdot \nabla T]_{\gamma,\ell,m} \tag{2.7}$$

$$\mathcal{D}_\ell \; (P_{\gamma,\ell,m}) = Pr \, R_s \, (6T_{\gamma,\ell,m} + r\partial T_{\gamma,\ell,m}/\partial r)$$

$$- r^{-2}\partial \, \{r[r \, \hat{e}_r \cdot (\underline{v}\cdot\nabla)\underline{v}]_{\gamma,\ell,m}\}/\partial r$$

$$- \{\nabla \cdot [(\underline{v} \cdot \nabla)\underline{v}]\}_{\gamma,\ell,m} \tag{2.8}$$

$$\mathcal{D}_\ell \; (\Phi_{\gamma,\ell,m}) = -3 \, Pr \, Rs \, T_{\gamma,\ell,m} \tag{2.9}$$

$$\langle \omega \rangle = \langle \psi \rangle = 0 \tag{2.10}$$

$$\frac{\partial \langle T\rangle}{\partial t} = r^{-2}\{\partial(r^2\partial\langle T\rangle/\partial r)/\partial r + \partial \mathcal{L}/\partial r$$

$$-\partial \, [\sum_{\gamma,\ell,m} r \, \ell(\ell+1) \, T_{\gamma,\ell,m} \, \omega_{\gamma,\ell,m}] / \partial r\} \tag{2.11}$$

where $\mathcal{D}_\ell$ is the differential operator defined by its action on the scalar, f:

$$\mathcal{D}_\ell (f) \equiv [\partial^2(rf)/\partial r^2 - \ell(\ell+1) f/r]/r \qquad (2.12)$$

and where $\mathcal{L}(r)$ is the luminosity

$$\mathcal{L}(r) = 4\pi \int_0^r \langle H \rangle r'^2 \, dr' \qquad (2.13)$$

In equations (2.5) - (2.11), $Rs \equiv \alpha G d^3 \mathcal{L}(d)/3k^2 \nu C_p$ is the Rayleigh number, $Pr \equiv \nu/k$ is the Prandtl number and γ stands for either R or I.

In equations (2.5) - (2.13) the unit of time is k/d^2, length is d, mass is ρd^3 and temperature is $\mathcal{L}(d)/4\pi\rho C_p dk$. Equations (2.5) - (2.10) may be thought of as the governing equations for each eddy or mode (γ,ℓ,m) that make up the total velocity field. The nonlinear terms in equations (2.5) - (2.13) such as $\{r\hat{e}_r \cdot [\underline{v} \cdot \nabla)\underline{v}]\}_{\gamma,\ell,m}$ are the eddy-eddy interaction terms, with contributions from all other pairs of modes (γ',ℓ',m') and (γ'',ℓ'',m'') that obey certain selection rules. The selection rules and the explicit expressions for the nonlinear interactions are given in a previous paper (Marcus 1979) in terms of Wigner-3j symbols. For a sphere with an impermeable, stress-free boundary the velocity is constrained at $r=1$ so that:

$$\omega_{\gamma,\ell,m}(1) = 0 \qquad (2.14)$$

$$\partial^2 \omega_{\gamma,\ell,m} / \partial r^2 |_{r=1} = 0 \qquad (2.15)$$

$$\partial(\psi_{\gamma,\ell,m} / r)/\partial r |_{r=1} = 0 \qquad (2.16)$$

We also require that the surface be isothermal:

$$T_{\gamma,\ell,m}(1) = 0 \quad . \tag{2.17}$$

We are free to choose the mean temperature to be zero at r=1:

$$<T(r=1)> = 0 \quad . \tag{2.18}$$

However, the gradient of the mean temperature (and therefore the flux) at r=1 is free to vary. The central temperature, $<T(0)>$, is also free to vary and is a measure of the efficiency of the overall convective flux. The lower the value of $<T(0)>$, the more isothermal the fluid is. The central temperature is given by

$$<T(0)> = -\int_0^1 \mathcal{L}/r^2 \, dr$$
$$- \int_0^1 \sum_{\gamma,\ell,m} \ell(\ell+1) \, T_{\gamma,\ell,m} \, \omega_{\gamma,\ell,m} \, /r \, dr$$
$$- \frac{\partial}{\partial t} \int_0^1 [\int_0^r r'^2 <T(r')> \, dr']/r^2 \, dr \tag{2.19}$$

We must use the central temperature as a measure of the efficiency convection because the Nusselt number is not well-defined for our boundary conditions.

3) Sufficient Conditions for a Good Truncation

The infinite set modal equations (2.5) - (2.13) for the coefficients can only be solved by arbitrarily setting some of the coefficients equal to zero (or some other functional form) and explicitly solving for the remaining finite set of coeffi-

cients. What are the consequences of setting some modes equal to zero? The equation for mean value of the temperature, (2.11), is well approximated, if and only if the term $\sum \ell(\ell+1)$ $\omega_{\gamma,\ell,m} T_{\gamma,\ell,m}$ /r, when summed over the finite set of kept modes, is nearly equal to what it would be if it were summed over all modes. Now, $\sum \ell(\ell+1) \omega_{\gamma,\ell,m} T_{\gamma,\ell,m}$ /r is equal to the convective flux and the contribution from each mode is just the convective flux carried by that particular eddy. Therefore equation (2.11) is well-approximated if we keep those eddies that carry most of the flux in the Galerkin expansion. Similarly it can be shown that equations (2.5) - (2.8) are well approximated only if we include the modes that are responsible for (1) the production of kinetic energy from buoyancy forces, (2) the production of the temperature variance, $1/2 \tilde{T}^2$, (3) the viscous dissipation of kinetic energy, (4) the dissipation of the temperature variance, (5) and those modes that provide the nonlinear cascade of energy from the production modes to the dissipative modes. We expect that the modes most responsible for production of the kinetic energy temperature variance and convective flux are the largest spatial modes. We also expect that if we wish to include all of the modes that are important in the cascade and dissipation of kinetic energy and temperature variance, we will have to retain all modes with Reynolds or Peclet numbers are greater than one.

C. The Effects of Truncations on the Kinetic Energy

The rate at which kinetic energy $\frac{\partial}{\partial t} \int \frac{1}{2} v^2 d^3r$ enters the fluids due to buoyancy is (Marcus, 1980a)

$$KE_{in} = 4\pi \ Pr \ Rs \int_0^1 \sum_{\gamma,\ell,m} \ell(\ell+1) \ T_{\gamma,\ell,m} \ \omega_{\gamma,\ell,m} \ r^2 \ dr \quad (2.20)$$

There are no cross-terms between different modes on the right-hand side of equation (2.20) and each term represents the kinetic energy contribution from one mode (ℓ,m,α). However, combining equation (2.11) with (2.20) shows us that we can write KE_{in} in terms of the luminosity and temperature gradient:

$$KE_{in} = 4\pi \ Pr \ Rs \int_0^1 \left[\frac{\partial \langle T \rangle}{\partial r} r^3 + r\mathcal{L} \right.$$
$$\left. - \frac{\partial}{\partial t} r \int_0^r r'^2 \langle T(r') \rangle \ dr' \right] dr \quad (2.21)$$

By numerical experimentation we have found that no matter how few modes are kept in the Galerkin expansion, the mean temperature gradient becomes nearly isothermal in the sense that

$$\left| \frac{\partial \langle T \rangle}{\partial r} \right| \ll \frac{\mathcal{L}(r)}{r} \quad (2.22)$$

Using equation (2.22) and taking the time-average (denoted by double brackets) of equation (2.21) we obtain:

$$\langle\langle KE_{in} \rangle\rangle \approx 4\pi \ Pr \ Rs \int_0^1 \mathcal{L}(r) \ r dr \quad (2.23)$$

We find that even the most severe truncations produce a close approximation to the correct value of $\langle\langle KE_{in} \rangle\rangle$.

The time-averaged value of the rate at which kinetic energy is dissipated, $\langle\langle KE_{out}\rangle\rangle$, must be equal to $\langle\langle KE_{in}\rangle\rangle$. KE_{out} is given by

$$KE_{out} = -4\pi \ Pr \int_0^1 \left[\left[r^{-1}\partial^2(rKE)/\partial r^2 \right.\right. \tag{2.24}$$

$$+ \sum_{\ell,m} \{-[\ell(\ell+1)]^2 \ r^{-2} \ \omega_{\gamma,\ell,m} \ \mathcal{D}_\ell \ (\omega_{\gamma,\ell,m})$$

$$-\ell(\ell+1) \ r^{-2} \ \partial(r\omega_{\gamma,\ell,m})/\partial r \ \partial[r \ \mathcal{D}_\ell \ (\omega_{\gamma,\ell,m})]/\partial r$$

$$\left.\left. - \ \ell(\ell+1) \ \psi_{\gamma,\ell,m} \ \mathcal{D}_\ell \ (\psi_{\gamma,\ell,m})\} \right]\right] r^2 dr$$

where $KE(r)$ is the kinetic energy of the fluid at radius r and is

$$KE(r) = \frac{1}{2} \sum_{\gamma,\ell,m} \ell(\ell+1) \left[\left[\left\{ \omega^2_{\gamma,\ell,m} \ \ell(\ell+1) \right.\right.\right.$$

$$\left.\left.\left. + \ [\partial(r\omega_{\gamma,\ell,m})/\partial r]^2 \right\}/r^2 + \psi^2_{\gamma,\ell,m} \right]\right] \tag{2.25}$$

Again, there are no cross terms between modes on the right-hand side of equation (2.24) and each term in the sum represents the dissipation due to one mode. If the high wavenumber modes responsible for the viscous dissipation are not included in the Galerkin expansion (or if the modes that are responsible for the cascade of kinetic energy to the dissipative modes are not included) $\langle\langle KE_{in}\rangle\rangle$ will not be strongly affected. However, to keep $\langle\langle KE_{out}\rangle\rangle$ equal to $\langle\langle KE_{in}\rangle\rangle$ the fluid must compensate by dissipating more kinetic energy in the large scale modes.

From equation (2.24) we see that one way in which the rate of dissipation can be increased is by increasing the kinetic energy of the modes. We therefore expect the kinetic energy of a severely truncated system to be abnormally high. This increase will be evident in the numerical examples in the next section.

D. The Effect of Truncation on the Fluctuating Thermal Energy

The rate at which temperature variance is created in the fluid is

$$TE_{in} = -4\pi \int_0^1 \frac{\partial <T>}{\partial r} r \sum_{\gamma,\ell,m} T_{\gamma,\ell,m} \omega_{\gamma,\ell,m} \ell(\ell+1) \, dr \quad (2.27)$$

Each term in equation (2.27) corresponds to the thermal input of one mode. Even though $|\frac{\partial <T>}{\partial r}|$ will generally be much less than $\frac{\ell}{r^2}$, we have found that for fixed Prandtl and Rayleigh numbers, $|\frac{\partial <T>}{\partial r}|$ can vary by an order of magnitude depending upon the number of modes kept in the Galerkin expansion. Therefore, $<<TE_{in}>>$ (unlike $<<KE_{in}>>$) is a sensitive function of the truncation. The rate at which the temperature variance is dissipated is

$$TE_{out} = -4\pi \sum_{\gamma,\ell,m} [(\partial T_{\gamma,\ell,m}/\partial r)^2 + \ell(\ell+1) \, r^{-2} T^2_{\gamma,\ell,m}] \, r^2 dr$$

$$(2.28)$$

If the Galerkin truncation does not include the thermally dissipative modes, the truncated solution will have to adjust itself so that $<<TE_{out}>>$ is kept equal to $<<TE_{in}>>$. The solu-

tion can increase the rate of thermal dissipation in the re-
tained modes by increasing the thermal variance of the modes.
However, unlike $\ll KE_{in}\gg$, $\ll TE_{in}\gg$ is not constrained and the
fluid can adjust to its inability to dissipate the thermal
variance by decreasing $\ll TE_{in}\gg$. Since $\ll TE_{in}\gg$ is propor-
tional to the mean-temperature gradient (eq. 2.27), the fluid
can reduce its rate of production of thermal variance by be-
coming more isothermal. In the next section we show numerical
examples in which a truncated solution both increases $\ll TE_{out}\gg$
by increasing its thermal variance and decreases $\ll TE_{in}\gg$ by
becoming more isothermal.

E. Single-Mode Theory

The severest truncation of a multi-mode expansion is to
retain only one horizontal mode. This requires that the solu-
tion be of the form:

$$T(r,\theta,\phi,t) = \langle T(r,t)\rangle + \tilde{T}(r,t)\, h\,(\theta,\phi) \qquad (2.29)$$

$$P(r,\theta,\phi,t) = \langle P(r,t)\rangle + \tilde{P}(r,t)\, h\,(\theta,\phi) \qquad (2.30)$$

$$\omega(r,\theta,t) = \tilde{\omega}(r,t)\, h\,(\theta,\phi) \qquad (2.31)$$

$$\psi = 0 \qquad (2.32)$$

where $h(\theta,\phi)$ is an eigenfunction of the horizontal Laplacian,
$(\nabla^2 - \frac{1}{r}\frac{\partial^2}{\partial r^2} r)$.

Because the toroidal modes are not involved in the convective
flux, kinetic energy production, or temperature variance produc-

tion they are neglected in single-mode theory. Our multi-mode numerical experiments have shown that the toroidal velocity is much smaller than the poloidal velocity except for large wave-number modes in large Rayleigh number convection. (See Marcus 1980b).

Unlike expansions with more than one horizontal mode, the single-mode solutions are always time-independent. Toomre et al. (1977),working with a plane-parallel geometry,also found that a single-mode always leads to a steady-state solution. Expansions with a single-mode suffer not only from the effects of truncation mentioned in the previous section, but also from other problems. For example, the correlation between the radial velocity and temperature,

$$\delta \equiv \langle \tilde{T} V_r \rangle / \langle \tilde{T}^2 \rangle^{1/2} \langle v_r^2 \rangle^{1/2} \qquad (2.33)$$

is always identically equal to 1 for a single-mode; whereas, experimentally, Deardorff and Willis (1967) have found that the correlation in air for Rayleigh-Bernard convection is between .5 and .7 for Rayleigh numbers between 6×10^5 and 10^7. The convective flux, $\langle T V_r \rangle$, that is far from the boundary predicted by single-mode theory is in good agreement with the flux predicted from multi-mode calculations (see §3). Because the single-mode over-estimates δ, it always underestimates $\langle \tilde{T}^2 \rangle \langle V_r^2 \rangle$, the product of the thermal variance and radial component of the kinetic energy. Another peculiarity of the single-mode equations is that the thickness of the boundary-layer at the surface is controlled by

viscosity and decreases as the Rayleigh number is increased (see Toomre et al. 1972) In a real fluid we would expect the boundary-layer to become turbulent and wide as the radially moving fluid smashes into the impermeable outer boundary. The thickness of the turbulent boundary-layer is not regulated by viscosity, but by the rate at which energy can be transferred to other modes. The increase in boundary-layer thickness due to the nonlinear cascade in a multi-mode calculation has been reported by this author elsewhere (1980a). In a single-mode calculation with a large Rayleigh number and an artificially thin boundary-layer, most of the dissipation of kinetic energy takes place near the surface with

$$<<KE_{out}>> \approx 4\pi P_r \int_{1-\chi}^{1} (\underline{v} \cdot \nabla^2 \underline{v})\, r^2\, dr \qquad (2.34)$$

where χ is the thickness of the boundary-layer. From equation (2.34) we see that $<<KE_{out}>>$ is proportional to $1/\chi$. Therefore, a single-mode calculation can compensate for its loss of dissipation in the missing high wavenumber modes by decreasing χ.

F. Lorenz Model

A further truncation of single-mode expansion gives us the Lorenz model. Using the equilibrium conductive temperature gradient with the single-mode equations, we can compute the complete set of orthonormal eigenmodes of the velocity and temperature (as functions of radius). By expanding the radial dependence of the velocity and temperature in terms of these eigenmodes, substituting the expansions into the single-mode equations and retaining only a single mode in the radial expansion, we obtain the Lorenz equations. These equations

were originally derived for a convecting fluid in a plane-parallel
geometry, but they can easily be extended to a spherical geometry.
The Lorenz model not only suffers from all of the physical approxi-
mations of single-mode theory but also contains some additional lia-
bilities. Because the functional form of the velocity and fluc-
tuating temperature are fixed and only their amplitudes are allowed to
vary, the fluid can never develop boundary-layers to help dissipate
the kinetic and thermal energy. More importantly, because the
functional form of the velocity and temperature are fixed, the
mean-temperature gradient can not become isothermal.

If we were interested in computing solutions only when the
Rayleigh number is slightly greater than its critical value, it
would be practical to expand the velocity and temperature in the
eigenmodes that are calculated with the conductive temperature gradient.
However, these are not a very useful set of functions in which to
expand the velocity and temperature when the Rayleigh number is
large. For example, for any large Rayleigh number, we can choose a
complete basis in which to expand the velocity and temperature by
calculating the fundamental and all of the higher harmonic solutions
to the single-mode equations. By retaining only the fundamental
mode in the expansion, a modified set of Lorenz-type equations is
obtained. We have computed the steady-state solutions to the
regular spherical Lorenz equation and to the new modified Lorenz
equations for a Rayleigh number $\sim$ 30 times greater than the criti-
cal value for the onset of convection. The solution to the regular
Lorenz equation is unstable with respect to time-dependent pertur-
bations; both the solution to the modified Lorenz equation and

the steady-state solution to the multi-mode equations with this Rayleigh number are stable. We conclude that qualitative description of the Lorenz model is not accurate for large Rayleigh numbers.

III. NUMERICAL RESULTS OF MULTI-MODE CALCULATIONS

In this section we present the numerical results of multi-mode calculations for Pr=10 and Rayleigh numbers of 10^4 and 10^5. For each Rayleigh number we repeat the calculation several times, each time using a different set of modes to show the effects of truncation. For all calculations, the heat source H(r) (see eq.2.13) is constant for r≤0.3 and zero elsewhere.

A. Rs = 10^4

To compute solutions to the modal equations, we have chosen the set of modes in the Galerkin expansion to be all of the spherical harmonics, $Y^{\ell, m}$ with $\ell \leq \ell_{cutoff}$, and all m. The radial dependence is finite-differenced with 128 grid points. For $\ell_{cutoff}=3,6,9$, and 12 we find that the solution is time-independent. A complete description of the solution with $\ell_{cutoff} = 12$ appears elsewhere (Marcus 1980a). To compare the overall features of the truncated solutions, we have listed the central temperature, KE_{in} and TE_{in} as a function of ℓ_{cutoff} in Table 3.1.

TABLE 3.1

ℓ_{cutoff}	<T(0)>	KE_{in}	TE_{in}
12	0.686	4.94×10^5	4.08
9	0.685	4.94×10^5	4.01
6	0.675	4.90×10^6	3.93
3	0.528	4.44×10^5	1.71

There is virtually no difference in the calculated values of $<T(0)>$, KE_{in} or TE_{in} for ℓ_{cutoff}=6,9, and 12, which indicates that modes with $\ell > 6$ are not important in production, transport or dissipation of energy. Using the value of KE_{in} from table 3.1, we find that the Kolmogorov length is ~ 0.212 which approximately corresponds to a wavenumber, ℓ, of ~ 4. The solution with ℓ_{cutoff}=3 shows the effects of truncation; the rate of input of thermal energy for ℓ_{cutoff}=3 is nearly 60% lower than it is for ℓ_{cutoff}=12. The rate KE_{in} for ℓ_{cutoff}=3 is nearly equal to KE_{in} for ℓ_{cutoff}=12. The large decrease in TE_{in} is consistent with the analysis presented in §2 which shows that the fluid can compensate for the loss of the thermally diffusive modes by decreasing TE_{in}. KE_{in} is constrained by the fact that it must always be approximately equal to $4\pi PrRs \int_{0}^{1} \mathcal{L}(r)r \, dr = 4.94 \times 10^{5}$. To compensate for the loss of the high wavenumber modes that dissipate the thermal variance when $\ell_{cutoff} = 3$, the fluid decreases TE_{in} by making the temperature gradient more nearly isothermal. The isothermal nature of the $\ell_{cutoff} = 3$ solution can be seen by noting that the central temperature for $\ell_{cutoff} = 3$ is less than it is for $\ell_{cutoff} = 12$.

A more sensitive probe of the effects of truncation is the kinetic and thermal energy spectra as functions of the horizontal wavenumber. In table 3.2 we have listed $TE(\ell, r=0.5)$, which is the 2-dimensional thermal variance spectrum at $r=0.5$, with wavenumber ℓ, i.e.

$$TE(\ell, r) = 2\pi \sum_{\gamma, m} (T_{\gamma, \ell, m})^2 r^2 \qquad (3.1)$$

We have also listed the kinetic energy spectra, $KE(\ell,0.5)$, at $r = 0.5$, as functions of ℓ and ℓ_{cutoff} in table 3.3. The kinetic energy spectra show that the value of $KE(\ell_{cutoff},0=.5)$ is higher than it should be. As pointed out in §3, the truncation causes an upward curl in the energy spectrum at ℓ_{cutoff} because the energy that cascades down from the large scale modes piles up at ℓ_{cutoff}. The upward curl at the large wavenumber end of the spectrum is even more pronounced in the thermal variance spectra. Because the Prandtl number is greater than unity, the dissipation of thermal energy is less efficient than the diffusion of kinetic energy. The thermal variance does not dissipate in the production modes as does the kinetic energy and is free to cascade down the spectrum and pile up at the large wavenumbers. For the severest truncation, $\ell_{cutoff} = 3$, the thermal energy spectrum has inverted itself and $TE(3,0.5) > TE(2,0.5) > TE(1,0.5)$.

B. $Rs = 10^5$

For a Rayleigh number of 10^5 and a Prandtl number of 10, we have computed solutions for $\ell_{cutoff} = 12,9,6,4,3,2$, and 1. With $\ell_{cutoff} = 1$ the solution is steady-state and the multi-mode equations reduce to those of single-mode theory. For a comparison between single and multi-mode solutions, we have plotted the kinetic energy of the $\ell = 1$ mode as a function of radius in figure 1 (solid line). Superimposed on this figure is the kinetic energy of the $\ell = 1$ mode (broken line) computed from the steady state solution of the multi-mode equation with $\ell_{cutoff} = 12$. The functional form of the two curves is quite similar,

the main difference being that the single-mode kinetic energy
is consistently higher than the multi-mode solution. This
difference in height confirms the predictions we made in §2:
the kinetic energy of the single-mode must be enhanced to in-
crease its rate of viscous dissipation. For the single-mode,
KE_{out} is 4.24×10^6, whereas for the $\ell = 1$ component of the
multi-mode solution, KE_{out} is only 3.13×10^6. Approximately
32% of the kinetic energy produced in the $\ell = 1$ component of
the multi-mode solution is lost not through dissipation but
through the nonlinear energy cascade.

In figure 2 we have plotted the temperature variance of
the $\ell = 1$ mode of the multi-mode solution (broken line) and
the single-mode solution (solid line). As in figure 1, the
two curves have the same function form, but, in general, the
single-mode thermal variance is greater than the multi-mode
variance. The greater thermal variance allows the single-mode
to increase its rate of thermal dissipation. The rates at
which the temperature variance is dissipated from the $\ell = 1$
component of the single- and multi-mode solution are 0.293 and
0.231 respectively.

For all solutions computed with $\ell_{cutoff} \geq 4$, the solutions
are steady-state and show truncation effects similar to those
found for $R_s = 10^4$. For $\ell_{cutoff} = 4$, the temperature spectrum is
inverted with $TE(\ell+1, 0.5) > TE(\ell, 0.5)$. The kinetic energy
spectrum is not inverted. In figure 3 we have plotted

$Q \equiv KE$ ($\ell=2$, $r=0.5$)/ $KE(\ell=3$, $r=0.3$) as a function
of ℓ_{cutoff}. Q is a measure of the upward curl of the kinetic
energy spectrum at $\ell=3$. If there were no truncation effects,
we would expect Q always to be greater than 1. If Q becomes
less than 1, it means that the kinetic energy spectrum is
inverted, i.e., $KE(\ell=3$, $r=0.5) > KE(\ell=2$, $r=0.5)$. Figure 3
shows that Q is greater than 1 but decreases as ℓ_{cutoff} decreases.
By extrapolating the points in figure 3, we may expect that Q is
less than 1 for $\ell_{cutoff}=3$. For $\ell_{cutoff}=3$ the solution is no
longer steady-state but is periodic in time. The kinetic energy
calculated with $\ell_{cutoff} = 3$ at $r=0.5$ as a function of wavelength,
ℓ, and as a function of time is plotted in figure 4 for one
period of the fluid's oscillation.

We have arbitrarily labelled the left-hand axis of figure
4 as $t=0$ but, in fact, it takes many iterations for the transients
in the fluid to settle down and for the motions to become per-
iodic. At $t=0$, the kinetic energy of the $\ell=1$. 2 and 3 wavelengths
are similar in value to the stationary values obtained with
$\ell_{cutoff}=12$. As time increases, the kinetic energy of $\ell=2$ and $\ell=3$
modes increases; they are unable to dissipate their kinetic energy
as fast as it cascades into (or is produced in)
the modes. At $t=.0467$ the kinetic energy of the $\ell=1$ modes
becomes less than that of the $\ell=2$ mode, and at
$t=.0503$ the kinetic energy of the $\ell=1$ and $\ell=3$ modes cross. At
this point in time, the kinetic energy spectrum changes quickly

and re-establishes the $\ell=1$ mode as the one with the largest
amount of kinetic energy. By $t=.152$, the solution settles down
from its rapid oscillations. The period of the energy spec-
trum is $t_p=.1528$, however, the period of temperature and velo-
city is $2t_p$. We have found that $\tilde{T}(t+t_p)=-\tilde{T}(t)$ and $\underline{v}(t+t_p)=$
$-\underline{v}(t+t_p)$. If we assume that the characteristic velocity of
the fluid is $[2\,KE\,(\ell=1,\,r=.5)|_{t=0}]^{1/2}$, then we can estimate
the eddy turnover time, t_e, to be $[2\,KE\,(\ell=1,\,r=5)|_{t=0}]^{-1/2}$
or 0.022. The period of the spectrum, t_p is 6.95 t_e. We
have repeated the calculation with $\ell_{cutoff}=3$ and with the
viscosity of the $\ell=3$ modes (but not the $\ell=1$ or 2 modes) increased
by 10%. With the enhanced viscosity the solution is steady-
state. When we increased the thermal diffusivity of the $\ell=3$
modes by 10%, the solution remained periodic in time.

With $\ell_{cutoff}=2$, the solution is both time dependent and
aperiodic. The solution wanders between a normal
and an inverted state. In the normal state $KE(\ell=1)\approx10^3$ and
$KE(\ell=2)\approx10$. In the inverted state $KE(\ell=1)\approx10^2$ and $KE(\ell=2)\approx10^4$.
The time dependence of the solution is reminiscent of the manner
in which a Lorenz solution wanders between two strange attrac-
tors. We have not attempted to determine whether there are
fixed points in the $\ell_{cutoff}=2$ equations of motion.

IV. DISCUSSION

We have calculated solutions to the equations of convection by expanding the horizontal structure in a series of modes. Choosing the number of modes to be retained in the solution is equivalent to fixing the spatial resolution in the horizontal direction. Keeping the number of modes fixed, we found that as the Rayleigh number increases, the solution changes in time from steady-state to periodic, and then to aperiodic. Alternatively, we have found that by keeping the Rayleigh number fixed at 10^5 and decreasing the number of modes, the solution changes from steady-state, to periodic, to aperiodic. In the extreme case where the expansion is limited to modes of only one horizontal wavenumber, the solution goes to a steady-state single mode. From our observations of the time-independent solutions with $R_s = 10^4$, we have found that truncating the horizontal expansion results in: 1) altering the kinetic and thermal spectra by increasing the amplitudes of the high wavenumber modes, 2) making the mean temperature gradient more isothermal and thereby lowering the central temperature, and 3) decreasing the rate at which the temperature variance is produced in the fluid. We have shown that if the truncation is too severe, the thermal variance spectrum will become inverted, with the high wavenumber dissipation modes having more energy than the low wavenumber production modes. The thermal variance inversion does not destroy the time-independent property of the fluid. We have shown in one example that if the truncation is severe enough that the kinetic energy spectrum is inverted, then the solution becomes time dependent. This suggests that we should be cautious

in numerically computing points of bifurcations in the flow
as a function of Rayleigh number alone. The points of bifur-
cations become curves of bifurcations when plotted both as a
function of Rayleigh number and limit of spatial resolution.

ACKNOWLEDGEMENTS

REFERENCES

Busse, F.H. (1978). Nonlinear Properties of Thermal Convection.
Reports on Progress in Physics, 41, 1929-1967.

Chandrasekhar, S. (1961). Hydrodynamic and Hydromagnetic
Stability. Oxford University Press.

Deardorff, J.W. & Willis, G.E. (1967). Investigation of
turbulent thermal convection between horizontal plates.
J. Fluid Mech. 28, 675-704.

Fenstermacher, P.R., Swinney, H.L., Benson, S.V. & Gollub, J.P.
(1978). Bifurcations to periodic, quasiperiodic, and
chaotic regimes in rotating and convecting fluids. In
Bifurcation Theory and Applications in Scientific Disciplines
(ed. O. Gurel & O.E. Rossler), New York Academy of Sciences.

Gough, D.O., Spiegel, E.A., and Toomre, J. (1975). Modal equa-
tions for cellular convection. J. Fluid Mech. 68, 695-719.

Lorenz, E.N. (1963). Deterministic nonperiodic flow. J. Atmos.
Sci. 20, 130-141.

McLaughlin, J.B. & Martin, P.C. (1975). Transition to turbulence
in a statistically stressed fluid system. Phys. Review A
12, 186-203.

Marcus, P.M. (1979). Stellar convection, I. Modal equations in
spheres and spherical shells. Ap.J. 231, 176-192.

Marcus, P.M. (1980a). Stellar Convection II: A Multi-Mode
Numeric Solution for Convection in Spheres. Submitted
to Ap. J.

Marcus, P.M. (1980b). Stellar Convection III: Convection at
Large Rayleigh Numbers. Submitted to Ap. J.

Ruelle, D. & Takens, F. (1971). On the Nature of Turbulence.
Commun. Math. Phys., 20, 167-192.

Toomre, J., Gough, D.O. & Spiegel, E.A. (1977). Numerical
Solutions of Single-Mode Convection Equations. J. Fluid Mech.,
79, 1-31.

FIGURE CAPTIONS

Figure 1 - The kinetic energy for the $\ell=1$ mode as a function of radius calculated with $\ell_{cutoff}=1$ (solid line) and $\ell_{cutoff}=12$ (broken line). The higher kinetic energy in the single-mode calculation allows more kinetic energy to be viscously dissipated and compensates for the inability of the single-mode calculation to lose energy by cascading.

Figure 2 - Same as figure 3 with the temperature variance of the $\ell=1$ mode plotted as a function of radius.

Figure 3 - $Q \equiv KE(\ell=2, r=0.5)/KE(3.r=0.5)$ as a function of ℓ_{cutoff}. Truncation causes the high wavenumber modes of the kinetic energy spectrum to become anomalously large. By extrapolation, it appears that when $\ell_{cutoff}=3$, $Q<1$ meaning that the kinetic energy spectrum has become inverted.

Figure 4 - The kinetic energy calculated with $\ell_{cutoff}=3$ at r=0.5 for the $\ell=1$, 2, and 3 modes as a periodic function of time. At t=.060? kinetic energy inverts so that $KE(\ell=1, r=.5) < KE(\ell=3, r=.5)$.

Figure 1

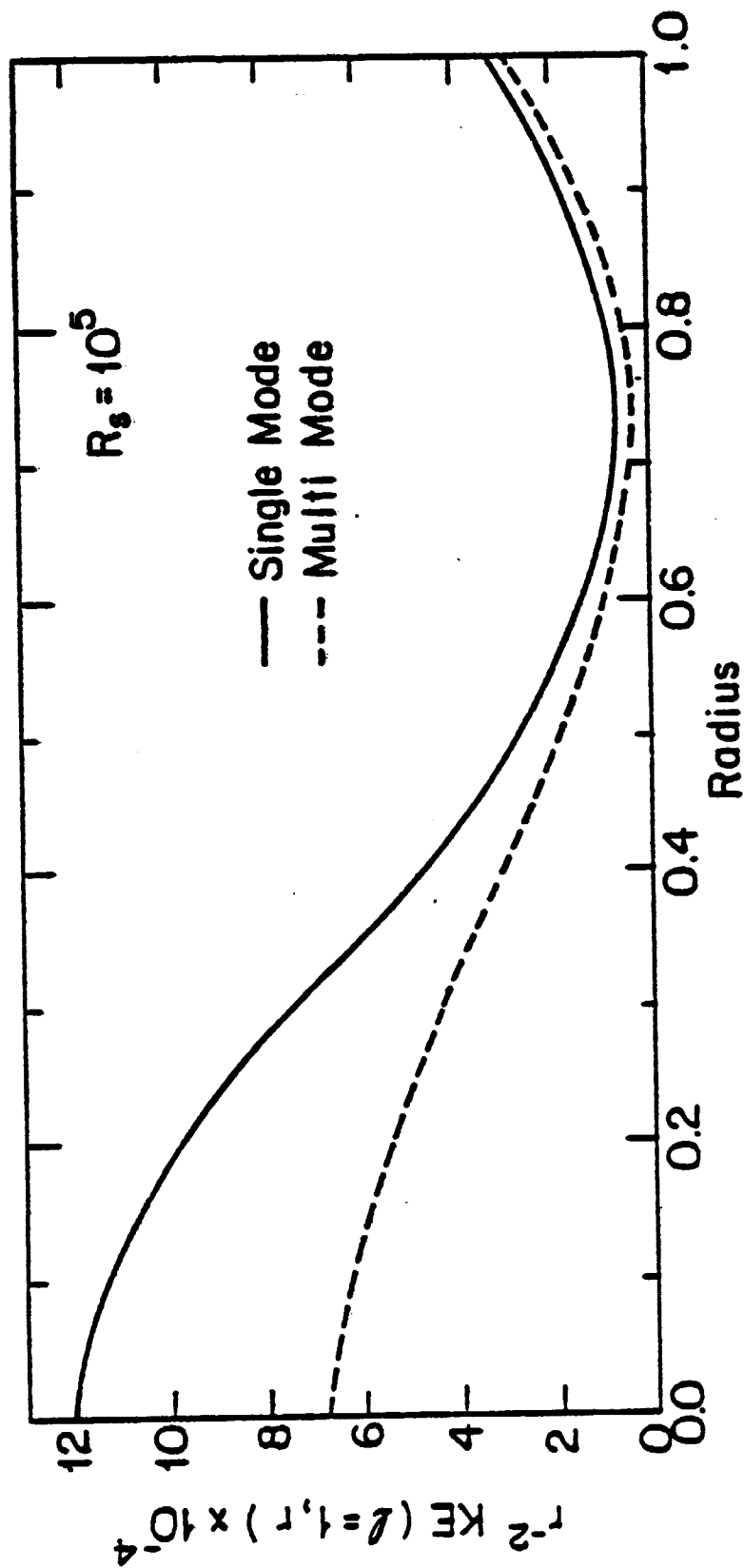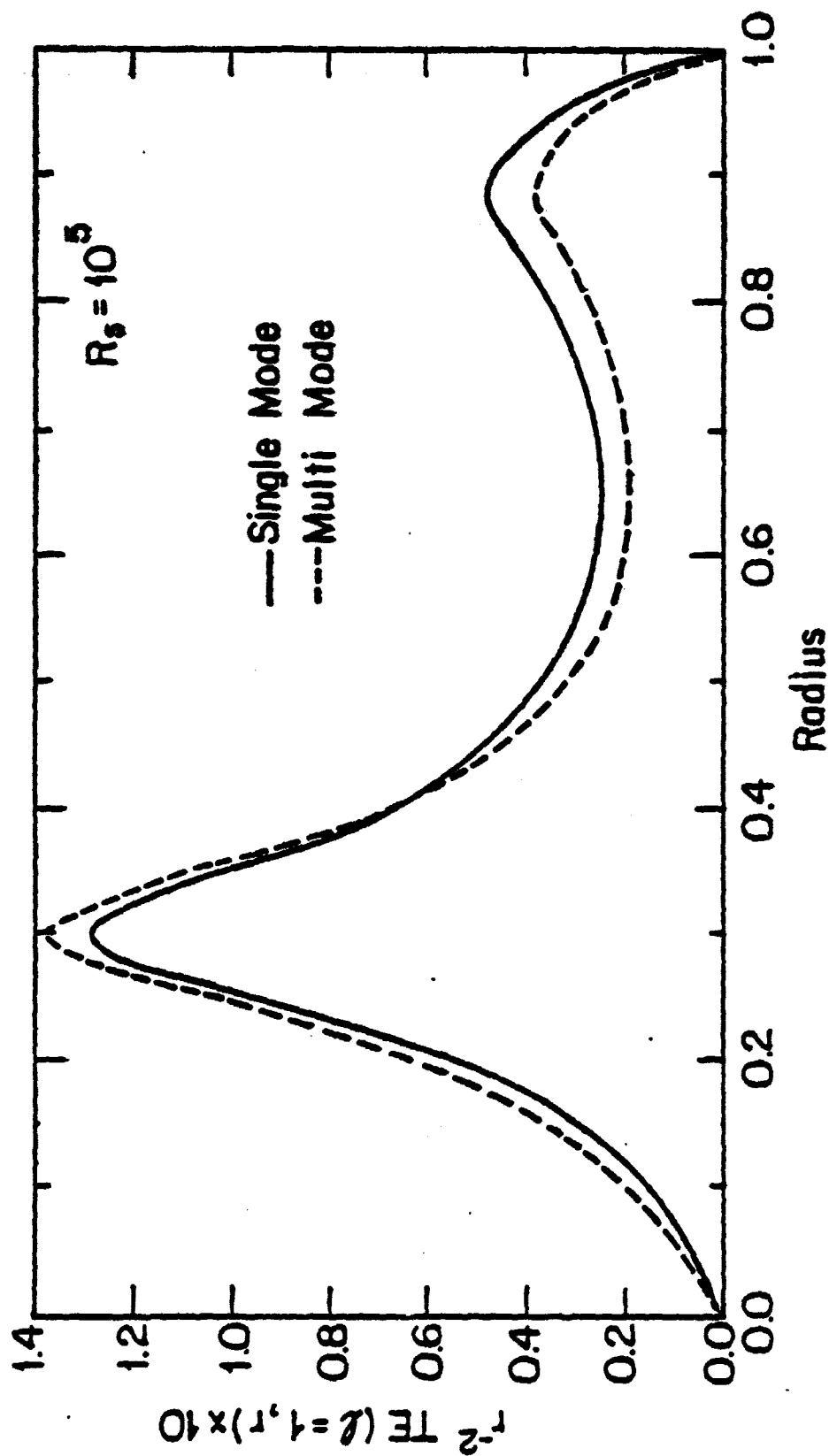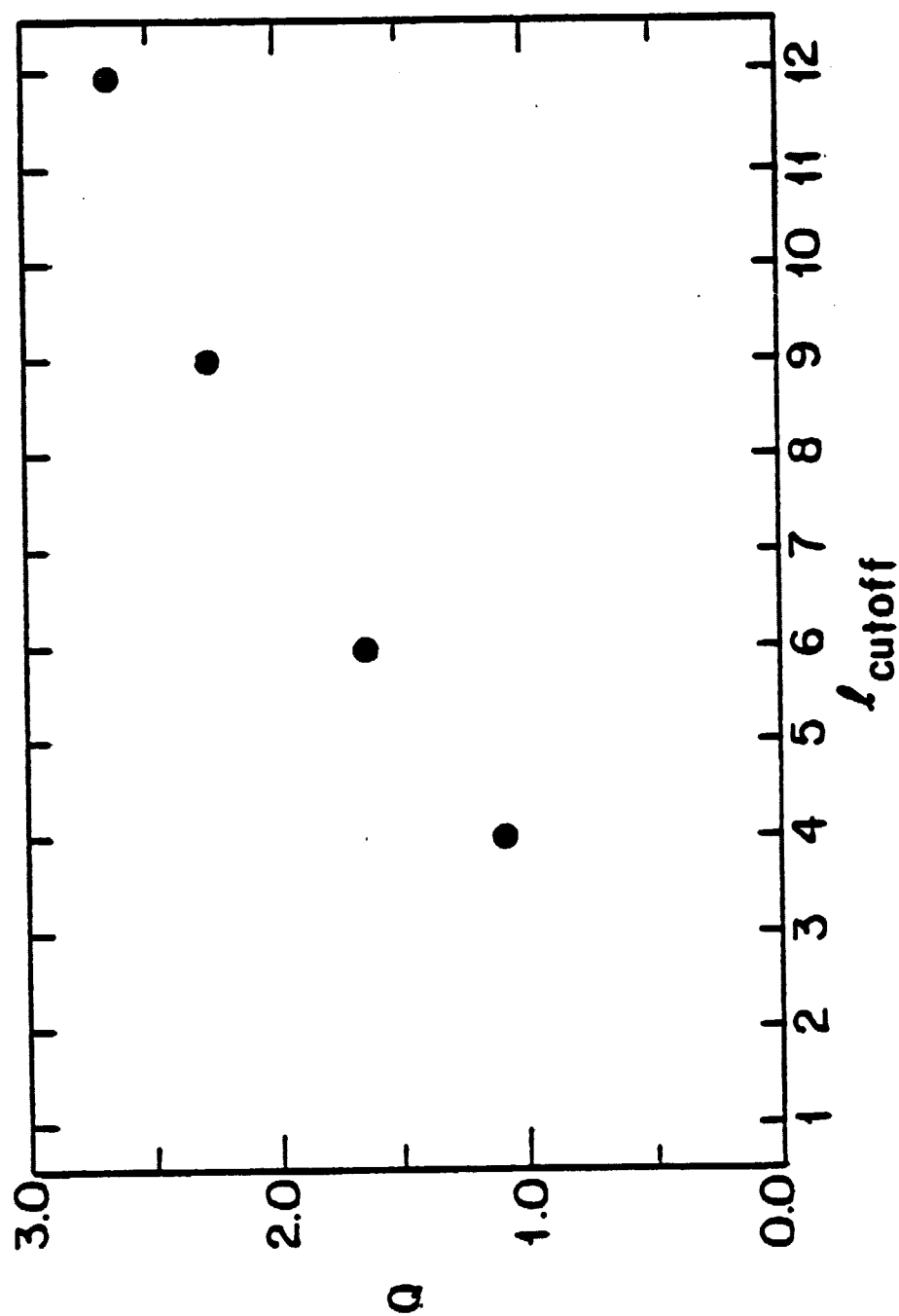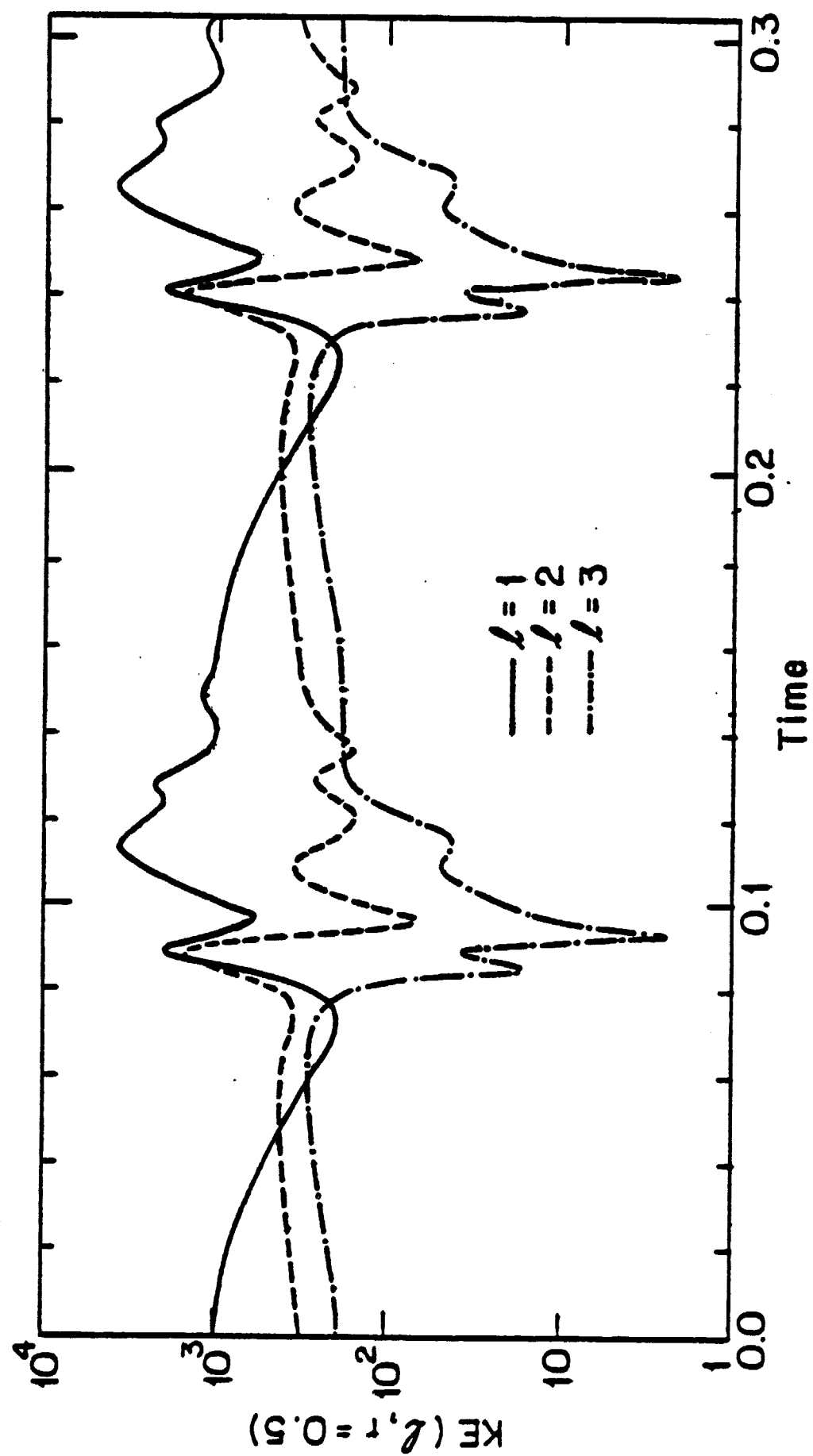Figure 2

Figure 3

Figure 4

AUTHOR'S ADDRESS

PHILIP S. MARCUS

CENTER FOR RADIOPHYSICS

AND SPACE RESEARCH

CORNELL UNIVERSITY

ITHACA, NEW YORK   14853